PNAS
www.pnas.org

Supplementary Information for

Arm movements induced by non-invasive optogenetic stimulation of the motor cortex in the common marmoset

Teppei Ebina, Keitaro Obara, Akiya Watakabe, Yoshito Masamizu, Shin-Ichiro Terada, Ryota Matoba, Masafumi Takaji, Nobuhiko Hatanaka, Atsushi Nambu, Hiroaki Mizukami, Tetsuo Yamamori, and Masanori Matsuzaki

Masanori Matsuzaki
Email: mzakim@m.u-tokyo.ac.jp

This PDF file includes:

www.pnas.org/cgi/doi/10.1073/pnas.1903445116

SUPPLEMENTARY METHODS

Animals

All experiments were approved by the Animal Experimental Committee of the University of Tokyo. Four laboratory-bred common marmosets (*Callithrix jacchus*) were used in the present study. The three marmosets (marmosets E, F, and G) used for photostimulation experiments were 6–7 months old (weight, approximately 260 g) when the habituation started. The marmosets were kept on a 12:12 h light-dark cycle and were not used for other experiments prior to the present study. An 89-month-old marmoset was used for the in situ hybridization experiment.

Head plate implantation

All surgical procedures and AAV injections were performed under aseptic conditions, as described previously (1). Marmosets were placed in a stereotaxic instrument (SR-5C-HT; Narishige, Tokyo, Japan) with anesthesia maintained using inhalation of isoflurane (1.5–4.0% in oxygen). Pulse oxygen (SpO_2), heart rate, and rectal temperature were continuously monitored. Cefovecin (14 mg kg^{-1}) as an antibiotic drug, and carprofen (3.75 mg kg^{-1}) as an anti-inflammatory drug to reduce pain and inflammation during and after surgery, were administered intramuscularly. Acetated Ringer's solution (10 ml) including riboflavin sodium phosphate (200 μg) was also administered subcutaneously. After *hair removal by a depilatory* and sterilization with povidone iodine, the skull was exposed. Lidocaine jelly was applied to wound sites to reduce pain. Five small screws were anchored to the skull, and a head plate (CFR-1; Narishige) was attached to the skull using dual-cured adhesive resin cement (Bistite II; Tokuyama Dental, Tokyo, Japan) following the application of a universal primer (Tokuyama Dental).

All experimental schedules are summarized in SI Appendix, Fig. S2 and S8B.

Animal training

One week after the plate implantation, we started to train marmosets E and F to perform forelimb (upper-limb) movement tasks according to the step-by-step protocol described previously (SI Appendix, Fig. S2; ref. 1). On training days, food and water were deprived to maintain the body weight at approximately 90% of normal weight. For each training session, a soft jacket was put onto the marmoset at the beginning and removed at the end of the session. In a self-initiated pole-pull task, the marmosets had to pull the pole above a reward threshold (15 mm) to obtain a 60–100 μl juice reward. Once the learning of this task was completed, the marmosets continued to perform it under head fixation. Next, in a visually cued pole-pull task, the head-fixed marmosets obtained a reward when they pulled the pole during a 3 s cued period indicated by a white square cursor appearing on the LCD monitor in front of the animal (Fig. 4A and 4B). The white cursor moved downward, depending on the position of the handling pole, with the color of the cursor turning to green when the pole

position exceeded a threshold. A blank period, during which no visual cue was drawn on the monitor, was inserted between the cued periods, and the marmosets were required to keep the pole below the threshold for 2–4 s. The training time in each session (day) of the visually cued pole-pull task lasted for more than 15 min for each marmoset after a month of training.

Marmoset G was trained in the self-initiated pole-pull task with the same protocol as described above, but before the head plate implantation. The metal plate implantation was then performed after the marmoset completed the task training (SI Appendix, Fig. S8B). After 1 week of recovery, the marmoset was trained to sit in the chair with head fixation but without performing any task. During the training, 16–40 μl of juice reward was given every 3–7 s. The training time in each session lasted for more than 25 min after 8 days of training.

The task devices were controlled by custom-made software written in LabView (National Instruments, TX, USA) and Visual C++ 2008 (Microsoft, WA, USA). The position of the pole was sampled at 1 kHz.

Identification of forelimb M1

After the training time under head fixation had reached more than 10 min, marmosets were placed in the stereotaxic instrument with isoflurane anesthesia, as described above. In marmosets E and F, an 11-mm diameter circular craniotomy with a center at 9.5–9.75 mm anterior from the interaural line and 4.5–5.0 mm lateral from the midline was performed, and the dura matter was removed; this site was presumed to be located above the primary motor cortex (M1; ref. 2, 3). The exposed cortex was filled with acetated Ringer's solution. A silver wire (diameter = 1.0 mm) was put on the skull near to the exposed cortex as the reference electrode. Then, the marmosets were moved to the task apparatus and the anesthesia was reduced. After recovery from the anesthesia (confirmed by checking eye opening, licking of the feeding tube, and arm movements), the marmosets usually started to pull the pole or sit in the apparatus sufficiently calmly to allow the ICMS to be performed for > 15 min. During the ICMS experiment, a drop of juice was given to the marmosets whenever they pulled the pole and every 30–60 s. In marmoset G, a rectangular craniotomy was performed over the putative M1 and PM (AP +4.5 mm to 16.5 mm, ML +1.0 to +9.0; ref. 2, 3), and the dura matter was removed. A silver wire with a diameter of 1 mm was put at the edge of the craniotomy and onto the remaining dura matter to act as the reference electrode (SI Appendix, Fig. S8A). The exposed cortex was covered with a 100-μm thick silicone membrane (6-9085-12, AS-ONE Corporation, Osaka, Japan) and silicone elastomer (Kwik-Sil; World Precision Instruments, FL, USA). Then, a plastic recording chamber (SI Appendix, Fig. S8A) was pressed onto the brain surface, and the space between the chamber and the brain surface was filled with the silicone elastomer. The edge of the chamber was then sealed with dental adhesive resin cement (Super bond; Sun Medical, Shiga, Japan) and the chamber was capped with a plastic cover consisting of a 3 × 5 mm glass coverslip (approximately 150 μm thickness;

Matsunami Glass, Osaka, Japan) attached to the bottom of the cover with UV-curing optical adhesive (LOCTITE 4305; Henkel, Vienna, Austria) (SI Appendix, Fig. S8A). The ICMS experiment was conducted 1 week after the surgery. During the experiment, a drop of juice was given to the marmosets every 5–7 s.

A tungsten microelectrode with an impedance of 0.5 MΩ (World Precision Instruments) was inserted to a depth of 1.8 mm from the cortical surface, and a train of 15 cathodal pulses (0.2 ms duration at 200 Hz) were applied. In marmosets E and F, the current was set to 10, 20, 30, 40, 50, or 100 μA. In marmoset G, the current was set to 10, 20, 30, 40, 50, 60, 70, 80 or 100 μA. The minimum current to elicit body part movements, as confirmed by two to three experimenters, was defined as the threshold current for that stimulation site. The type of the body part movement (extension, flexion, or rotation) was determined by the visual inspection of the experimenters. Cortical areas that had a relatively low movement threshold in comparison with more posterior or anterior areas, and/or that induced body movements with a threshold less than or equal to 30 μA for marmosets E and F, or 10 μA for marmoset G, were considered as M1. The reason why the threshold currents for marmosets E and F were larger than that for marmoset G and other report (4) might be because the ICMS experiments in marmosets E and F were conducted on the same day as the craniotomy, after recovery from the anesthesia.

Virus production

The AAV vector for AAV1-CaMKII-Cre was obtained from the University of Pennsylvania Gene Therapy Program Vector Core (Cat#AV-1-PV2396). The AAV vector for pAAV-Thy1S-tTA was described previously (5). The vector plasmid for pAAV-TRE-flex-ChR2 (E123T/T159C)-EYFP was constructed by replacing the Ef1a promoter of pAAV-Ef1a-DIO hChR2(E123T/T159C)-EYFP (Addgene #35509) with the TRE3 promoter of pTRE3G-ZsGreen1 (Takara/Clontech, Shiga, Japan). The vector plasmid for pAAV-TRE-flex-Clover was constructed by insertion of two pairs of incompatible lox sites under the Tet response element (TRE), and Clover (a variant of GFP; ref 6) was inserted inversely between the lox sites.

Virus injection

A pulled glass or quartz pipette (broken and beveled to approximately 30-μm outer diameter; Sutter Instruments, CA, USA) and a 5-μl Hamilton syringe were back-filled with mineral oil (Nacalai Tesque, Kyoto, Japan) and front-loaded with virus solution consisting of AAV1-CaMKII-Cre (2.3×10^{12} vg/ml), AAV1-Thy1S-tTA (0.15×10^{12} vg/ml), and AAV1-TRE-flex-ChR2 (E123T/T159C)-EYFP (1.1×10^{12} vg/ml). The ChR2 variant E123T/T159C has fast channel kinetics (7). The pipette was inserted vertically at 1.8 mm ventral from the surface of the identified M1, PM, and area 3a. The total amount of 500 nl of AAV cocktail was injected at a rate of 0.1 μl min^{-1} for 5 min with a syringe pump

(KDS310; KD Scientific, MA, USA), with the pipette then being maintained in place for an additional 5 min before being slowly withdrawn. A window consisting of a 4.5 (for marmoset E) or 5.5 mm (for marmoset F) circular glass coverslip (approximately 150 μm thickness; Matsunami Glass) attached to the bottom of a titanium chamber (height, 1.2 mm) with UV-curing optical adhesive was pressed onto the brain surface, and the space between the chamber and the brain surface was filled with silicone elastomer. The edge of the chamber was sealed with dental adhesive resin cement. As the metal head plate was attached to the head before the ICMS experiment in marmoset E, the anterior side of the plate was located near to the identified M1. Therefore, the titanium chamber was placed slightly to the back of the forelimb M1 area, and several ICMS sites were not included within the glass window (SI Appendix, Fig. S1A).

Optogenetic stimulation of the forelimb M1

A 450 nm laser (BioRay 450; Coherent, CA, USA) was delivered through a 0.05-mm core multi-mode fiber (N.A., 0.22; M15L02; Thorlabs, NJ, USA) and collimating lens (f = 7.86 mm, F240FC-532; Thorlabs; SI Appendix, Fig. S1A). The laser beam was then expanded with two-tandem lenses (f = 15.0 and 10.5 mm, LA1540-A and ACL1210U-A; Thorlabs) to a diameter of approximately 2 mm centered on the wrist area identified by ICMS (SI Appendix, Fig. S1A). To provide laser beam illumination with a diameter of 1 mm (SI Appendix, Fig. S3 and the mapping experiments), the laser was delivered through the multi-mode fiber and a collimating lens (f = 2.0 mm, PAF2-2A; Thorlabs).

More than 1 week after the virus injection, we restarted to train marmosets E and F in the visually cued pole-pull task, and marmoset G to sit in the chair without performing the task. After an additional 1–2 weeks, we tested whether the high-power laser photostimulation could induce arm movements during the training. M1 was photostimulated in 44 and 6 sessions for marmosets E and F, respectively, with the cursor reaching the reward threshold in 11.6–100.0% (median, 87.0%) and 86.5–98.6% (median, 95.5%) of trials, respectively. After 1–1.5 months post-injection, we found that the photostimulation induced visible changes in the cursor trajectory. In marmoset G, after 1-month post-injection, we found visible hand movement while the animal sat in the chair. The waiting periods for the movement induction corresponded to 48–50 days from the virus injection, a period that is necessary for optogenetic induction of single unit activity in awake marmosets (8). As the photostimulation parameters such as the frequency and light pulse width varied in every experiment, and the high-power laser illumination induced large hand movements overwhelming the pole-pull movement, we did not include the data from these sessions in the present analyses.

Marmosets E and F were also trained to sit in the apparatus without the pole-pull task, but with reward deliveries at intervals of 4–10 s. The marmosets were able to sit calmly for more than 15 min without performing a task, even in the first training session (17.1 and 15.2 min for marmosets E and F, respectively). In these periods, 5 ms laser pulses were illuminated five times at 100 Hz, five

times at 10 Hz, or 50 times at 100 Hz. For analysis of the hand movements and electromyograms (EMGs) evoked by the photostimulation, the stimulation was applied approximately 20 and 100 times respectively, with the marmosets showing no large arm movements. The timing of the stimulation was decided by the experimenters. The interstimulation interval ranged from 0.6 to 34.6 s and the laser power at the stimulation site was set to 3.8 (low), 21.1 (middle), or 38.0 mW (high). Marmoset E underwent 26 training sessions without the pole-pull task but with the photostimulation, and marmoset F underwent 27 such sessions. Of these, 15 sessions for marmoset E and 15 sessions for marmoset F were not analyzed because of variation in the stimulation parameters, inappropriate CCD camera positions, the hand positions during the photostimulation being too large to predict (the hand moved outside the CCD camera imaging field), the maximum distance between the original hand positions across trials being larger than 50 mm, or the EMG signals having high noise levels.

For motor mapping, a custom-made XY scanning stage placed below the marmoset chair was moved to an appropriate position to move the 1-mm diameter photostimulation spot. For each site, 50 or 500 ms photostimulation with a laser power of 38.0 mW was applied 7–25 times with an interstimulation interval of > 1 s. In marmosets E and F, 16 stimulation sites were set within the cranial window (SI Appendix, Fig. S7). In marmoset E, the circular window was replaced with a 4.2 × 8.2 mm rectangular window. In marmoset G, a window consisting of a 9 × 5 mm rectangular glass coverslip was attached to the bottom of a plastic chamber (height, 1.2 mm) with UV-curing optical adhesive, and 67 stimulation sites were set (Fig. 3). In marmoset G, 500 ms photostimulation with a laser power of 8.4 mW was also applied. For each stimulation parameter, the stimulation series was repeated for one to three sessions and the trial-averaged hand and elbow movements were analyzed. The mapping experiments were conducted for four, three, and six sessions in marmosets E, F, and G, respectively.

To examine the modulation effect of the photostimulation on voluntary forelimb movement, fifty 5-ms-pulse photostimuli were applied at 100 Hz during performance of the visually cued pole-pull task described above. These pulsed photostimuli were applied at −1500, −500, 0, or +500 ms from the cue onset. Each photostimulation timing was randomly assigned to 16.7% of the trials in each session (50% of trials had no photostimulation). In the task sessions before this experiment, the ratios of the number of beyond-threshold pole-pull events during the cued period to those during the cued period and during the blank period (hit rate) were 83.8% and 77.8% in marmosets E and F, respectively. The laser power was set to 0.5–1.2 mW, so as not to induce visible forelimb movement. We measured the mean values of the Z-axial pole positions before the cue onset (−1500 to 0 ms) and removed trials with values outside the median ± 3 median absolute deviations (MAD) within the same stimulation condition. Thirteen and five training sessions with the 0.5–1.2 mW stimulation were performed on marmosets E and F, respectively. Of these, ten sessions from marmoset E and one session from marmoset F were not analyzed because of a hit rate less than 70%, with the marmosets

frequently releasing the pole, the mean cursor position before the cue onset being too close to the reward threshold (less than ~5 mm from the threshold), photostimulation timing not being fixed, or pole positions before the photostimulation being significantly different from those in the no-stimulation trials.

Monitoring and prediction of hand movements

Two CCD cameras (DMK33GP1300; ImagingSource, Taipei, Taiwan) equipped with fixed-focus lenses (focal length, 3.0 mm; #89-341; Edmund, NJ, USA) were orthogonally set 190 mm to the left side and 175 mm in front of the marmoset. During the photostimulation experiments, two 480 × 480 pixel CCD images were simultaneously obtained at 100 frames per second (a resolution of 0.3 mm per pixel at the hand position). The exposure time for each frame was set to 2.5 ms.

The marmosets' hand positions were predicted with DeepLabCut version 1.0 (https://github.com/AlexEMG/DeepLabCut; ref. 9). For each session, we extracted the images recorded with the front CCD camera across −300 to +1500 or −500 to +1500 ms from photostimulation onset. From these recordings, we randomly selected 100 images and manually marked the positions of the left hand (back of the base of the middle finger), elbow, and shoulder in each image. Using these marked images, we then trained DeepLabCut with 400 000 iterations and predicted their positions across the whole of the extracted images. In addition to the position, DeepLabCut also exported the likelihood score of the prediction, which represented the similarity of the posture of the marmoset in the test image to that in the training images. Trials with a likelihood score less than 0.95 (the score ranged from 0.0 to 1.0) were removed, as predictions below the threshold score usually indicate incorrect target positions (e.g., predicted a position on the task apparatus with high light-reflection intensity as the hand, probably because the hand positions in the training datasets sometimes had high light-reflection intensity, as shown in Fig. 2A). We calculated the displacement of the hand positions to analyze the amplitude of the hand movements induced by the photostimulation. To do this, we extracted the predicted XY-coordinate of the hand positions from the images and measured the hand displacement, which was the distance between the position at each time point and the average position across −300 to 0 ms of the stimulation onset in the same trial (original position). For the 50 ms photostimulation, the amplitude was calculated as the mean displacement across 0 to +200 ms from the stimulation onset. For the 500 ms photostimulation, it was calculated across 0 to +500 ms. As the trials with significant differences in hand displacements between the periods from −300 to −150 and −150 to 0 ms would involve spontaneous hand movements, these trials were not included in the analysis. For the mapping analysis, trials with significant differences in hand displacements between the period from −300 to 0 ms and the period from 0 to 500 ms were used. Significance was measured using the Wilcoxon rank-sum test with a P-value threshold of 0.05. For presentation of the trajectories of the shoulder, elbow, and hand positions,

only trials with a likelihood score > 0.95 for all positions were used. Thus, the number of presented trials differed between Fig. 2B left and right, and between Fig. 2C left and right. The YZ-coordinate of the positions was also calculated from the images obtained with the left-side CCD camera (SI Appendix, Fig. S5).

EMG recording and analysis

EMG was recorded from biceps, triceps, extensor, and flexor muscles with a pair of surface silver electrodes with a diameter of 1 mm (Unique Medical, Tokyo, Japan) and a separation of 2 mm. An adhesive paste (Elefix; NIHON KOHDEN, Tokyo, Japan) was used to attach the electrodes to the skin covering one of the target muscles. The surface EMG (sEMG) signals were amplified and filtered from 10 to 2000 Hz through a differential amplifier (EX1; DAGAN, MN, USA), and were archived by a NI-DAQ device (National Instruments) with a sampling rate of 10 kHz. The signals were then full-wave rectified, filtered with a Gaussian filter (σ = 1.0 ms), and down sampled to 1 kHz. The mean of the EMG signals during the pre-stimulation period was measured, and the trials with a mean value outside ± 3 MAD were removed, because these trials were considered to be those with large spontaneous sEMGs. The sEMGs were compared within the non-overlapping 10 ms bins across the time from 0 to 100 ms from the stimulation onset.

Histology

Marmoset E was deeply anesthetized by an intraperitoneal injection of sodium pentobarbital and perfused transcardially with 0.9% NaCl followed by fixation with 4% paraformaldehyde (PFA) in 0.1 M phosphate-buffered saline (PBS, pH 7.4). The brain was removed and put into 4% PFA for 3 days at 4°C. The brain was then embedded in 3% agar in PBS and sliced coronally into 100 μm sections with a vibratome (VT-1000S, Leica Biosystems, Nussloch, Germany). For immunohistochemistry, the sections were incubated in PBS containing 10% normal goat serum (NGS) for 1 h at 4°C, and then with mouse anti-parvalbumin antibody (1:1000, Swant, Marly, Switzerland) in PBS containing 2% Triton X-100 at 4°C overnight. Sections were washed three times with PBS, and incubated with fluorescence conjugated secondary antibody (Alexa 594 conjugated anti-mouse IgG, 1:100) in PBS for 5 h at 4°C. To localize cell nuclei, sliced sections were incubated in PBS containing 2 μg/ml propidium iodide (Nacalai Tesque, Kyoto, Japan) and 2% Triton X-100 at 4°C for 30 min. The sections were mounted on glass slides with ProLong Diamond Antifade Mountant (Thermo Fisher Scientific, MA, USA). Images (318.2 × 318.2 μm) were obtained with a confocal microscope (A1R, Nikon, Tokyo, Japan). Cells were defined as EYFP-positive when their cytosol had strong EFYP fluorescence, or their cell membrane was clearly visible with the fluorescence.

One marmoset received a cocktail of AAV1-CaMKII-Cre (2.3×10^{12} vg/ml), AAV1-Thy1S-tTA (0.15×10^{12} vg/ml), and AAV1-TRE-flex-Clover (1.1×10^{12} vg/ml) to determine the ratios of

excitatory and inhibitory neurons to the transgene-positive cells in our expression system. Compared with ChR2, which is transported to the membrane, it is much easier to identify the cell bodies of the Clover-positive cells. We performed immuno-in situ hybridization using an antibody for GFP that also recognizes Clover, combined with VGLUT1 or GAD67 gene probes, which detect the cell bodies of the excitatory and inhibitory neurons, respectively (10). Immuno-in situ hybridization was performed as described previously (11). Briefly, 20-μm sections were obtained using a freezing microtome (Retratome REM-710, Daiwa-Koki, Saitama, Japan), and were used for hybridization with the DIG-labeled gene probes. After hybridization, the Clover-positive cells were identified by a chick antibody to GFP (ab13970, Abcam, MA, USA), whereas the hybridized DIG-labeled probes were detected by alkaline-phosphatase reaction with an HNPP Fluorescent Detection Set (Sigma-Aldrich, MO, USA). The fluorescent images were acquired using a confocal microscope (Fluoview FV-1000, Olympus, Tokyo, Japan) with a 20× objective. Images of 200 × 200 μm were set for counting. To judge the colocalization of the GFP and gene probes for the nearby neurons, we also considered whether the shapes of the positive neurons matched. This measure was sometimes necessary to distinguish adjacent cells that were tightly packed together.

We observed the transgene expression in approximately 10% of the inhibitory neurons, which likely reflects the endogenous ratio of the inhibitory neurons. This was not surprising, because although CaMKII promoter is generally considered to be an excitatory-specific promoter, it has been known to drive transgene expression in inhibitory neurons in AAV viral expressions (e.g., ref. 5, 12, 13). Furthermore, even highly inhibitory-specific Dlx promoter is reported to lose its specificity when combined with the Cre system (14).

Statistics

Statistical analyses were performed using MATLAB (R2016a, 9.0.0.341360; MathWorks, MA, USA). Wilcoxon's rank-sum test and the Kruskal-Wallis test followed by a post-hoc Dunn-Sidak test were used for statistical comparisons. No statistical tests were run to predetermine the sample size. Data are presented as mean ± SEM, unless otherwise noted. Blinding and randomization were not performed.

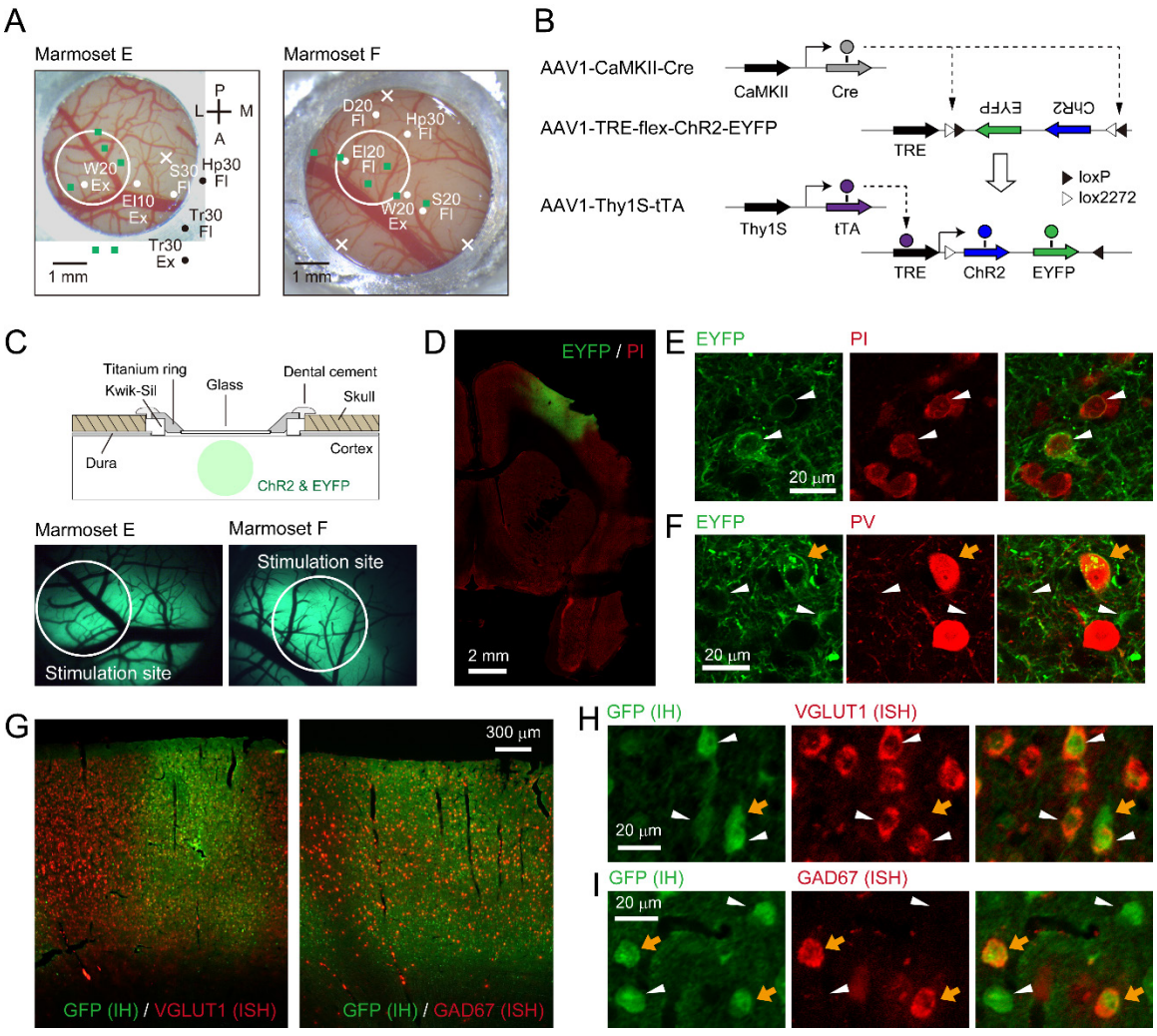

Figure S1. ChR2 expression in the marmoset motor cortex.

(A) M1 cortical surface through a glass window. White and black dots indicate the ICMS sites that induced visible body movements. The numbers and characters next to the dots represent the threshold current required to induce the movements and the moved body parts with their movement type, respectively. D, digit; W, wrist; El, elbow; S, shoulder; Tr, trunk; Hp, hip. Ex, extension; Fl, flexion; Rt, rotation. Crosses indicate the sites at which ICMS with ≤ 50 μA stimulation current induced no movement. Green squares indicate the AAV injection sites. The white circle indicates the photostimulation area with a diameter of 2 mm, as also shown in (C). (B) Scheme of the TET-inducible system for ChR2 expression in marmoset M1. Cre inverts the floxed segment encoding ChR2-EYFP, and the ChR2-EYFP is expressed in neurons when tTA binds to the TRE3 promotor in the absence of doxycycline. (C) Top, scheme of the glass window. Bottom, epi-fluorescence images from the same imaging window shown in (A) on post-injection days 92 (marmoset E) and 57 (marmoset F). (D) Coronal slice including the motor cortex of marmoset E. EYFP fluorescence and

cell nuclei stained with propidium iodide (PI) are shown in green and red, respectively. (E) Representative EYFP-expressing cells (green, arrowheads) and cell nuclei (red) around the injection site. (F) A representative EYFP-expressing cell (green) that co-expresses parvalbumin (PV; red; orange arrows) and cells that do not (white arrowheads). (G) Example slices of the cortex of a marmoset that received injections of AAV-Thy1S-tTA, CaMKII-Cre, and TRE-flex-Clover. Clover (GFP) was detected by immunostaining (IH; green) and VGLUT1/GAD67 mRNA expressions were detected by in situ hybridization (ISH; red). (H) A representative Clover-expressing cell (green) that does not co-express VGLUT1 (orange arrows) and cells that do (red; white arrowheads). (I) Representative Clover-expressing cells (green) that co-express GAD67 (red, orange arrows) and cells that do not (white arrowheads). Orange arrows in (F, H, and I) indicate inhibitory neurons that express the transgene.

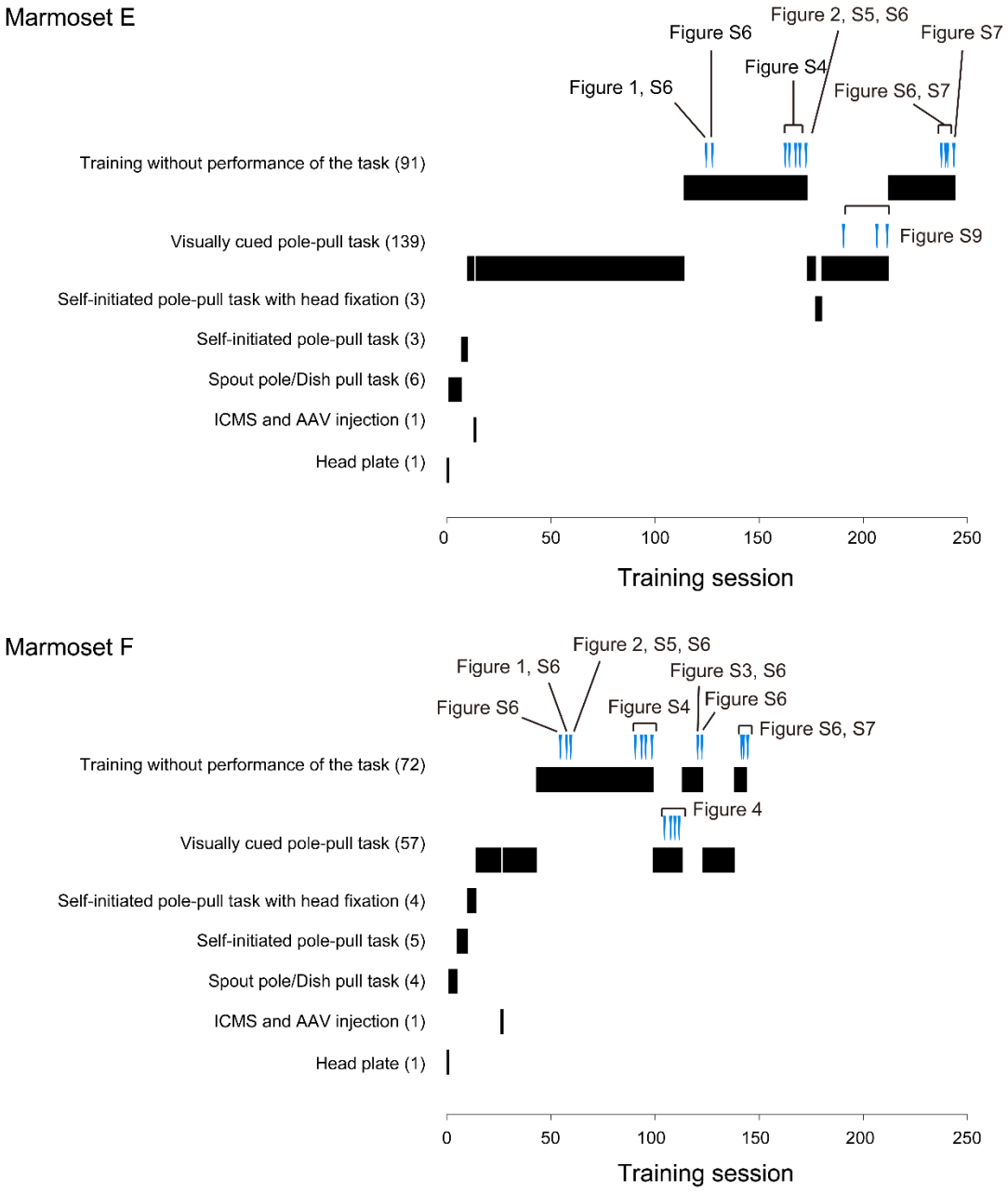

Figure S2. Task schedules for marmosets E and F.

Black bars indicate the training sessions for the tasks indicated on the left. The top three tasks were performed with head fixation. The numbers on the left labels indicate the total number of sessions for the corresponding task. Blue arrowheads indicate the sessions in which the data were analyzed for the indicated figures. Days without behavioral experiments are not included, and all sessions on the left labels are concatenated. The details of each task are described in ref. 1.

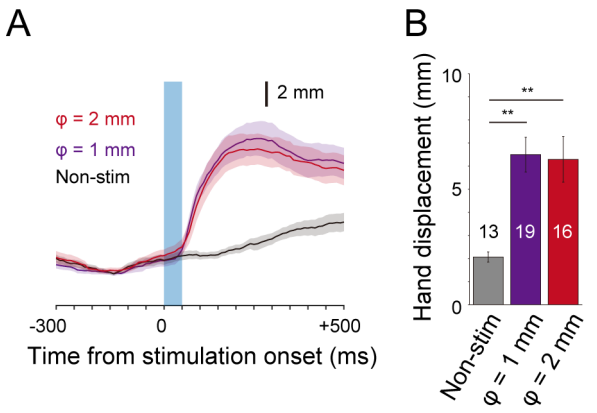

Figure S3. Photostimulation of the M1 area (1-mm diameter) induced hand movements.

(A) Displacement of the hand position in marmoset F. Red and purple lines represent the trial-averaged displacements induced by photostimulation of the areas with spot diameters of 2 and 1 mm, respectively. The stimulation center was the same. Black lines are the trial-averaged displacements in the non-stimulation trials. Shaded areas represent the SEM. The blue box indicates a 50 ms duration with five 5 ms duration pulses of blue laser light (450 nm, 38 mW) illuminated at 100 Hz. All data were obtained in the same session. (B) The amplitude of hand displacement at the different stimulation areas. Bars represent mean ± SEM. **P < 0.01 (Kruskal-Wallis test followed by Dunn-Sidak post-hoc test).

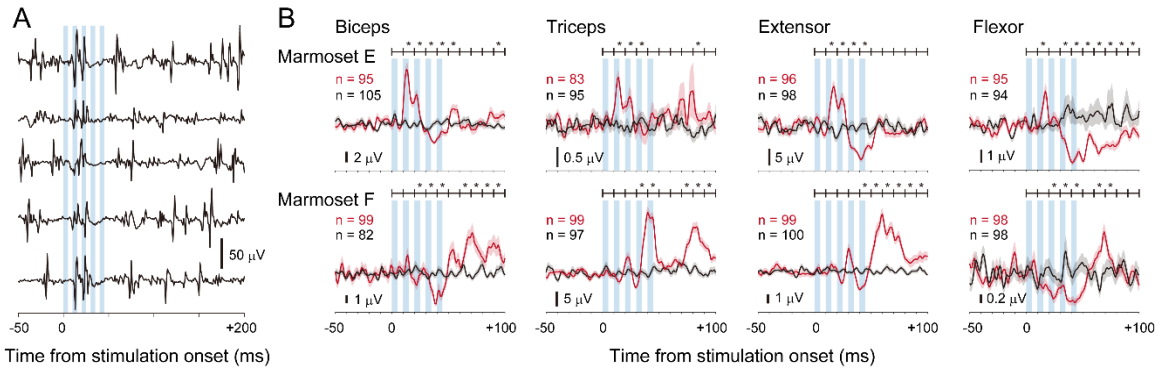

Figure S4. M1 photostimulation evokes surface EMG (sEMG) responses in four arm muscles.
(A) Examples of the sEMG recordings from the biceps muscle of marmoset E in five photostimulation trials with high laser power (38.0 mW). Blue-shaded areas indicate the timing of the photostimulation. (B) sEMGs from four arm muscles in two marmosets. Red and black lines represent the averaged sEMGs during trials with and without photostimulation, respectively. Shaded areas represent the SEM. *P < 0.05 (Wilcoxon rank-sum test between the amplitude of the sEMGs in trials with and without photostimulation).

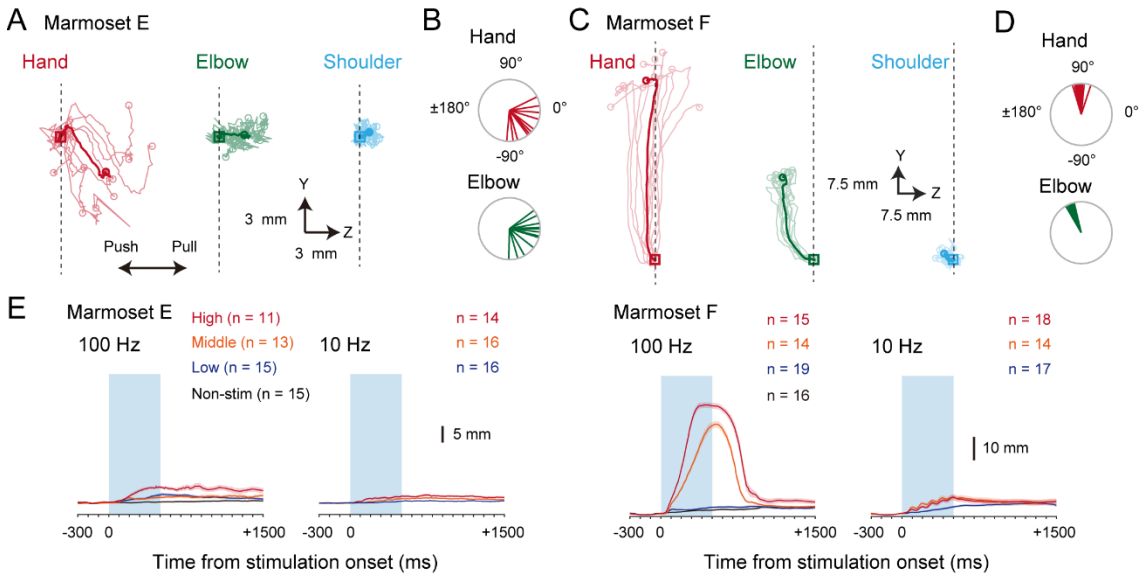

Figure S5. YZ-coordinates of the hand, elbow, and shoulder positions in images from the left-side CCD camera.

(A) Trajectories of the hands (red), elbows (green), and shoulders (blue) of marmoset E across −300 to +500 ms from stimulation onset (n = 9 trials). The sessions are the same as those in Fig. 2. Each trajectory is aligned to its original position. Shaded and solid lines represent the individual and trial-averaged trajectories, respectively. Squares and circles indicate the original and end positions, respectively. The positive Z-direction is the pull direction. (B) Distribution of the direction of the hand (red) and elbow (green) movements in (A). (C, D) The same plots as in (A, B), but from marmoset F (n = 11 trials). (E) Trial-averaged YZ-displacements of hand position induced by the photostimulation with different stimulation strengths at 100 and 10 Hz frequencies. The session was the same across (A–E) for each marmoset. The number of presented trials differed between Fig. 2B left and SI Appendix, Fig. S5A, and between Fig. 2C left and SI Appendix, Fig. S5C, because these images were acquired with different (front and left-side) cameras.

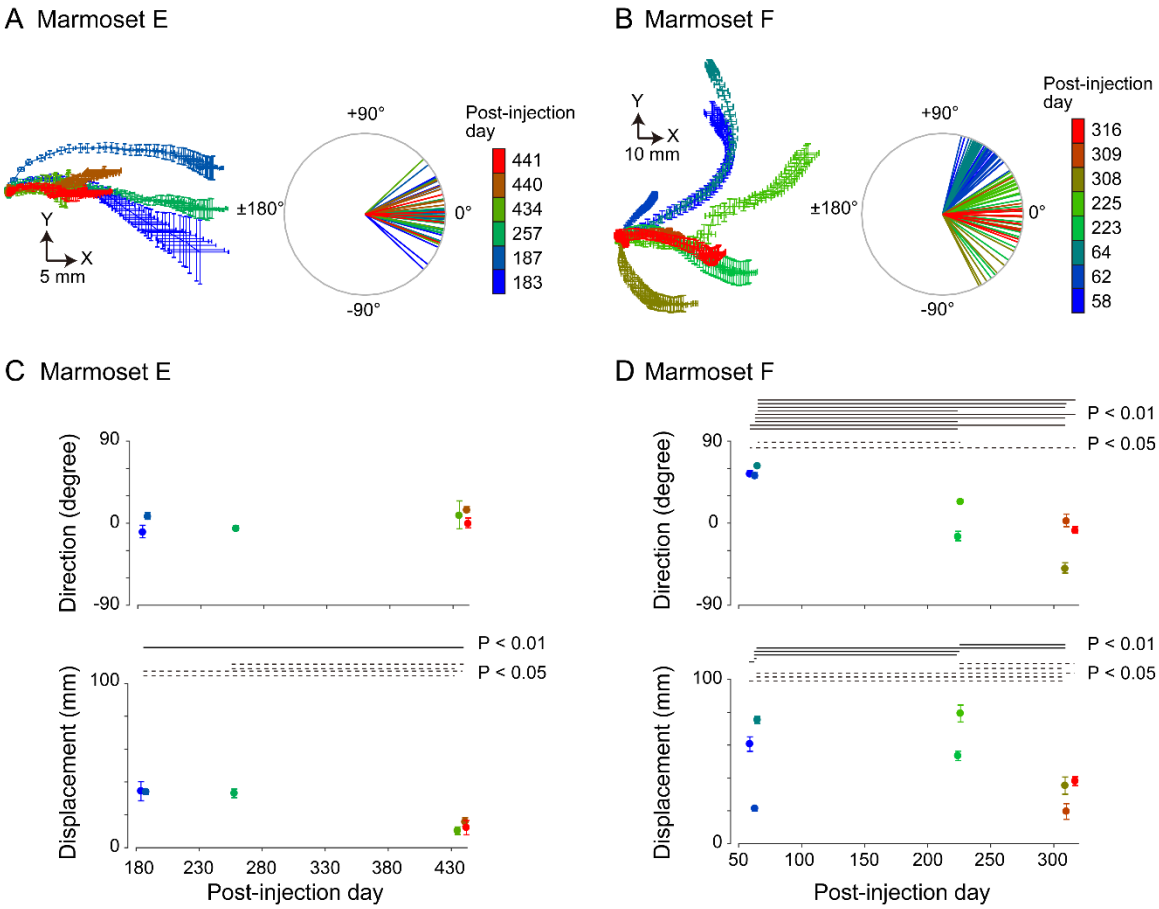

Figure S6. Stability of hand movement trajectories across sessions.

(A, B) XY-coordinates of hand movement trajectories induced by 500 ms photostimulation in marmosets E (A) and F (B). Left, trial-averaged trajectories of movements relative to their original positions. The positions every 10 ms are shown. Error bars represent SEMs. The trajectories are color coded according to the post-injection day as indicated on the right. Middle, distribution of the movement direction angles. Each line represents the direction angle of the movement in each trial. (C, D) Mean movement direction angle (top) and displacement (bottom) from the original to end positions in each session in marmosets E (C) and F (D). Solid and dotted lines at the top of each panel indicate statistical values of < 0.01 and < 0.05 (Kruskal-Wallis test with Dann-Sidak post-hoc correction), respectively, in the comparison between the sessions at the end points of the corresponding lines.

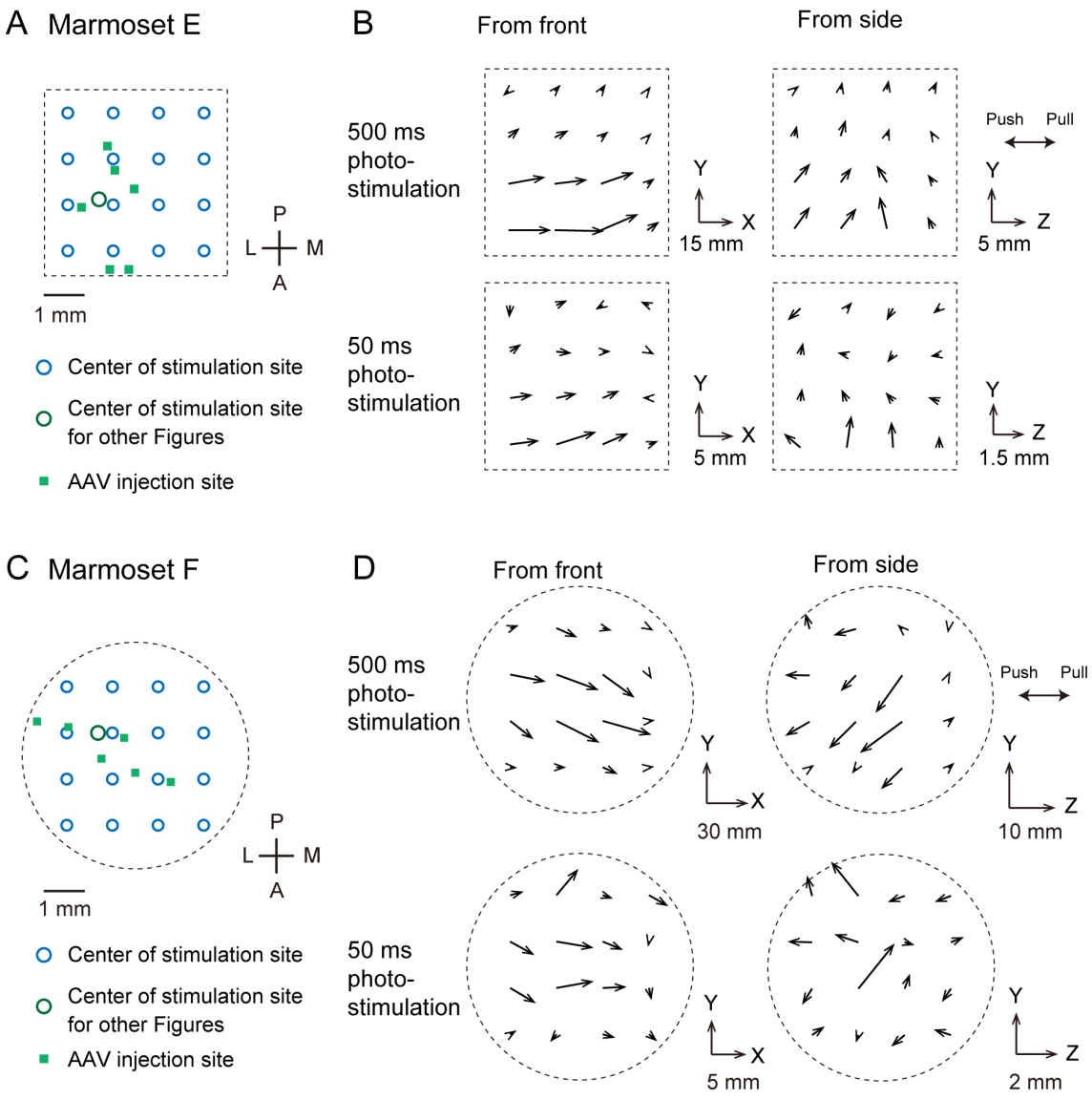

Figure S7. Motor mapping by photostimulation in marmosets E and F.

(A) Photostimulation sites within the cranial window in marmoset E. Blue circles indicate the center of stimulation spots. The green circle indicates the center of the stimulation site for other figures. Green squares indicate the virus injection sites. In marmoset E, the circular cranial window was replaced with a 4.2 × 8.2 mm rectangular window to map the virus-injected sites outside the original cranial window (SI Appendix, Fig. S1A). (B) Direction and displacement of the movements between the original and end points of the trial-averaged hand movements in marmoset E. The direction and the displacement correspond to the direction and length of the arrow, respectively. The positive X-, Y-, and Z-directions are lateral, upward, and pull directions, respectively. (C and D) The same plots as in (A and B), respectively, but for marmoset F. The conventions are the same as in (A and B).

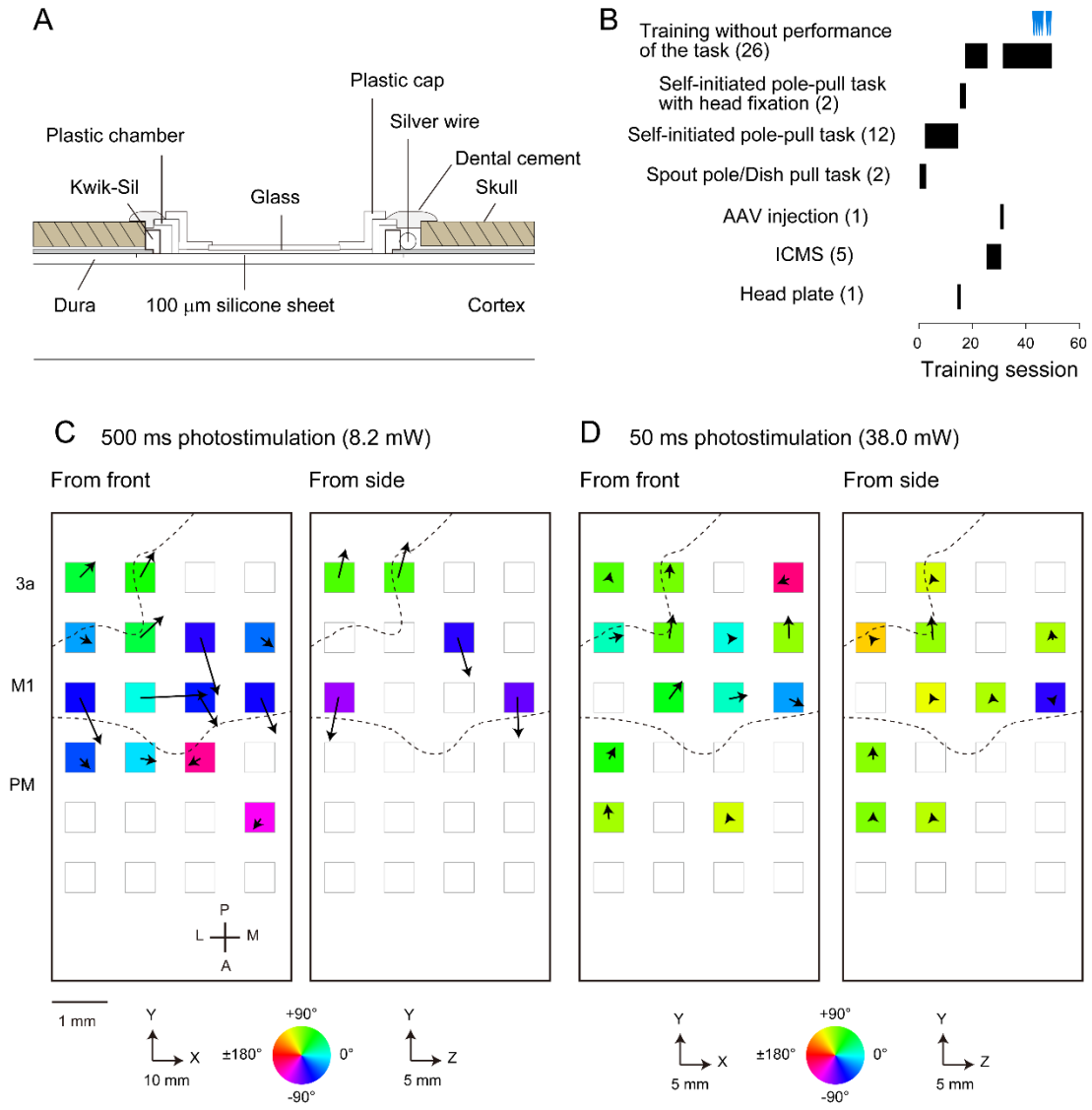

Figure S8. Mapping experiments in marmoset G.

(A) Schematic illustration of the recording chamber for repetitive ICMS mapping over five sessions within a week. At the beginning of each experiment, the plastic cap was removed, and the tungsten electrode was inserted through the silicone sheet. (B) Task schedule. The conventions are the same as in SI Appendix, Fig. S2. Blue arrowheads indicate the sessions in which the data were analyzed in Fig. 3D–G and SI Appendix, Fig. S8C and S8D. (C and D) Large-field maps of the hand movement direction and displacement due to the photostimulation with middle–low power of 8.2 mW and repetitive photostimulation duration of 500 ms (C), and with high laser power of 38.0 mW and short repetitive photostimulation duration of 50 ms (D). Conventions are the same as in Fig. 3D. In both experiments, there were 24 photostimulation sites. Only stimulation sites with a movement displacement of ≥ 4.0 mm (C) or ≥ 1.0 mm (D) are represented by color and arrows.

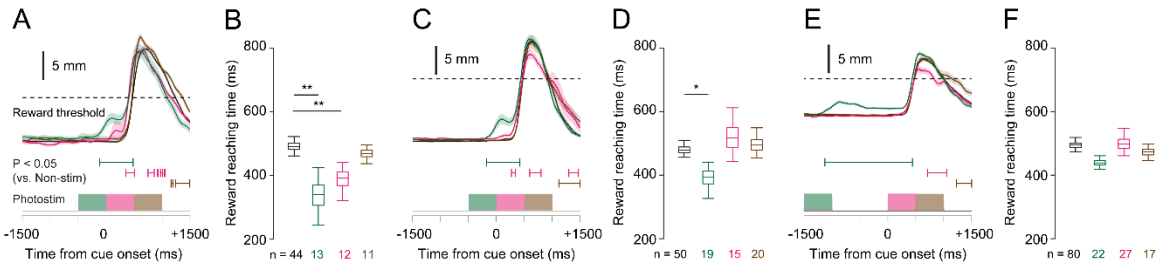

Figure S9. Perturbation of forelimb movements by M1 photostimulation in marmoset E during performance of a visually cued pole-pull task.

(A) Traces of the Z-axial pole position during tasks with and without photostimulation. The conventions are the same as in Fig. 4C. (B) Reward reaching time in each trial type in (A). The conventions are the same as in Fig. 4D. (C, D) Traces of Z-axial pole position (C) and reward reaching time (D) in a different session from (A). (E, F) Traces of Z-axial pole position (E) and reward reaching time (F) in the session in which the pre-cue stimulation was applied at −1500 ms from cue onset. *P < 0.05, **P < 0.01 (Kruskal-Wallis test with Dann-Sidak post-hoc correction).

SI REFERENCES

1. Ebina T, et al. (2018) Two-photon imaging of neuronal activity in motor cortex of marmosets during upper-limb movement tasks. Nat. Commun. 9:1879.
2. Hardman CD, Ashwell KWS (2012) Stereotaxic and Chemoarchitectural Atlas of the Brain of the Common Marmoset (*Callithrix jacchus*). (CRC Press, Boca Raton, FL).
3. Yuasa S, Nakamura K, Kohsaka S (2010) Stereotaxic Atlas of the Marmoset Brain. (Igaku Shoin, Tokyo).
4. Wakabayashi M*, et al.* (2018) Development of stereotaxic recording system for awake marmosets (*Callithrix jacchus*). *Neurosci. Res.* 135:37-45.
5. Sadakane O*, et al.* (2015) Long-term two-photon calcium imaging of neuronal populations with subcellular resolution in adult non-human primates. *Cell Rep.* 13:1989-1999.
6. Lam AJ*, et al.* (2012) Improving FRET dynamic range with bright green and red fluorescent proteins. *Nat. Methods* 9:1005-1012.
7. Berndt A*, et al.* (2011) High-efficiency channelrhodopsins for fast neuronal stimulation at low light levels. *Proc. Natl. Acad. Sci. USA* 108:7595-7600.
8. MacDougall M*, et al.* (2016) Optogenetic manipulation of neural circuits in awake marmosets. *J. Neurophysiol.* 116:1286-1294.
9. Mathis A*, et al.* (2018) DeepLabCut: markerless pose estimation of user-defined body parts with deep learning. *Nat. Neurosci.* 21:1281-1289.
10. Komatsu Y, Watakabe A, Hashikawa T, Tochitani S, Yamamori T (2005) Retinol-binding protein gene is highly expressed in higher-order association areas of the primate neocortex. *Cereb. Cortex* 15:96-108.
11. Watakabe A, Komatsu Y, Ohsawa S, Yamamori T (2010) Fluorescent in situ hybridization technique for cell type identification and characterization in the central nervous system. *Methods* 52:367-374.
12. Nathanson JL, Yanagawa Y, Obata K, Callaway EM (2009) Preferential labeling of inhibitory and excitatory cortical neurons by endogenous tropism of adeno-associated virus and lentivirus vectors. *Neuroscience* 161:441-450.
13. Scheyltjens I*, et al.* (2015) Evaluation of the expression pattern of rAAV2/1, 2/5, 2/7, 2/8, and 2/9 serotypes with different promoters in the mouse visual cortex. *J. Comp. Neurol.* 523:2019-2042.
14. Dimidschstein J*, et al.* (2016) A viral strategy for targeting and manipulating interneurons across vertebrate species. *Nat. Neurosci.* 19:1743-1749.